CHEMBIOCHEM

DOI: 10.1002/cbic.200800502

Photocontrollable Peptide-Based Switches Target the Anti-Apoptotic Protein Bcl-x_L

Sabine Kneissl,[a] E. Joel Loveridge,[a] Christopher Williams,[b] Matthew P. Crump,[b] and Rudolf K. Allemann*[a]

Photocontrol of Bcl-x_L binding affinity has been achieved by using short BH3 domain peptides for Bak_{72-87} and Bid_{91-111} alkylated with an azobenzene crosslinker through two cysteine residues with different sequence spacings. The power to control the conformation of the crosslinker and hence peptide structure was demonstrated by CD and UV/Vis spectroscopy. The binding affinity of the alkylated peptides with Bcl-x_L was determined in their dark-adapted and irradiated states by fluorescence anisotropy measurements, and use of different cysteine spacings allowed either activation or deactivation of the binding activities of these peptide-based switches by application of light pulses. Helix-stabilized peptides exhibited high Bcl-x_L binding affinity with dissociation constants of 42±9, 21±1, and 55±4 nM for Bak_{72-87}^{i+7}, Bak_{72-87}^{i+11}, and Bid_{91-111}^{i+4}, respectively (superscript numbers refer to the spacing between cysteine residues), and up to 20-fold enhancements in affinity in relation to their helix-destabilized forms. Bak_{72-87}^{i+7}, Bak_{72-87}^{i+11}, and Bid_{91-111}^{i+4} each displayed more than 200-fold selectivity for binding to Bcl-x_L over Hdm2, which is targeted by the N-terminal helix of the tumor suppressor p53. Structural studies by NMR spectroscopy demonstrated that the peptides bind to the same cleft in Bcl-x_L as the wild-type peptide regardless of their structure. This work opens the possibility of using such photocontrollable peptide-based switches to interfere reversibly and specifically with biomacromolecular interactions to study and modulate cellular function.

Introduction

Physical interactions between proteins underpin all cellular processes and provide opportunities for new research tools and medicines. Despite the obvious importance of intracellular protein–protein interactions, they have proven inherently difficult to target with small-molecule chemistry, due to the fact that protein interfaces are extensive, shallow, and mainly hydrophobic, making them relatively uniform molecular landscapes with only limited opportunities for selective chemical intervention. Protein surfaces have hence often been described as "nondruggable".[1–4] The development of peptide-based reagents that mimic nature's strategy for protein recognition provides an alternative, nature-like strategy to target protein–protein interactions selectively.[5–17]

The B-cell leukaemia-2 (Bcl-2) family of proteins constitutes a critical control point for the regulation of programmed cell death. Family members such as Bcl-x_L and Bcl-2 inhibit apoptosis, are over-expressed in many cancer cells and are involved in tumor initiation and progression as well as resistance to therapy.[18,19] Other family members including Bak and Bid can act as promoters of apoptosis.[20,21] The sensitivity of cells to apoptotic stimuli has been shown to depend on the fine balance between pro- and anti-apoptotic proteins, which is mediated by their heterodimerization.[22] Members of the Bcl-2 family are characterized by the presence of up to four conserved Bcl-2 homology (BH) domains that contain α-helical peptide segments. The solution structure of the complex of Bcl-x_L with a short 16 amino-acid peptide derived from the BH3 region of Bak revealed that the Bak peptide forms an amphipathic helix, which binds to a hydrophobic groove on the surface of Bcl-x_L formed by the juxtaposition of Bak's BH1, BH2, and BH3 domains.[23] Peptides derived from BH3 domains bind to Bcl-x_L with high nanomolar to low micromolar affinities, and the α-helicity of such peptides is known to be critical for high-affinity binding.[24]

Inhibitors of the interaction of pro- and anti-apoptotic members of the Bcl-2 family not only have significant potential as therapeutics but should also facilitate the study and regulation of the complex cellular processes leading to cell death or tumor growth. Although several potent small-molecule and peptide-based inhibitors of the Bcl-x_L/Bak interactions have been developed recently,[5–7,25–35] none of these provides the ability to program changes in discrete and critical intracellular protein–protein interactions through external stimuli in a reversible manner.

We have previously described a strategy for using light to control the DNA binding affinities and specificities of the transcription factor MyoD and of HDH-3, which is a miniature protein derived from the homeobox protein engrailed.[34,35] This

[a] S. Kneissl, Dr. E. J. Loveridge, Prof. R. K. Allemann
School of Chemistry, Cardiff University
Main Building, Park Place, Cardiff, CF10 3AT (UK)
Fax: (+44) 29-2087-4030
E-mail: allemannrk@cf.ac.uk

[b] Dr. C. Williams, Dr. M. P. Crump
School of Chemistry, University of Bristol
Cantock's Close, Bristol, BS8 1TS (UK)

Supporting information for this article is available on the WWW under http://www.chembiochem.org or from the author.

approach relies on the introduction of an azobenzene crosslinker through appropriately spaced cysteine residues. Photoisomerization of the crosslinker can be used to switch peptides between the α-helical and random coil-like conformations[34–42] (Figure 1) and has also been applied to control of the conformation of β-hairpins.[43–45] Significant stabilization of the α-helical conformation was observed when the crosslinker was in the *cis* configuration for peptides linked through cysteine residues in *i*, *i*+7 and *i*, *i*+4 spacings, while the *trans*-configuration was helix-stabilizing for *i*, *i*+11 spacing.[34–37] Here we demonstrate the versatility of such photocontrollable peptide-based switches for the control of protein–protein interactions and report highly potent and specific examples that target the anti-apoptotic protein Bcl-x_L.

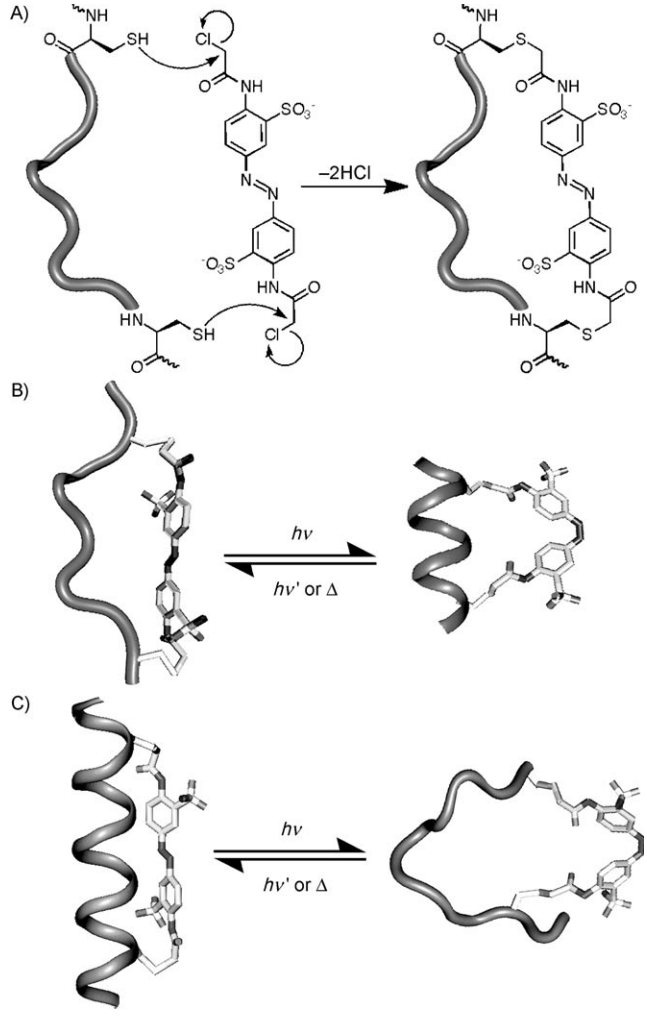

Figure 1. A) Modification of a peptide with the azobenzene crosslinker to form a photocontrollable peptide-based switch. B) Structural change upon isomerization of the azobenzene crosslinker attached to a peptide in an *i*, *i*+7 spacing. The same structural change is observed with the crosslinker in an *i*, *i*+4 spacing, except that only one helical turn is stabilized. C) Structural change upon isomerization of the azobenzene crosslinker attached to a peptide in an *i*, *i*+11 spacing.

Results and Discussion

Design of photocontrollable peptides

Two Bak-based peptides—Bak_{72-87}^{i+7} and Bak_{72-87}^{i+11}—based on the structure of the Bcl-x_L/Bak_{72-87} complex[23] were designed. Two appropriately spaced residues on the solvent-exposed face of the Bak_{72-87} helix, opposite the residues involved in Bcl-x_L-binding,[23] were replaced with cysteines (Figure 2) to allow for the introduction of the photo-activatable crosslinker 3,3′-bis(sulfo)-4,4′-bis(chloroacetamido)azobenzene. The superscript numbers in the peptide names indicate the spacings of the cysteine residues. Gln73 was changed to cysteine in Bak_{72-87}^{i+11} and to alanine in Bak_{72-87}^{i+7}. Asp84 was substituted by cysteine in Bak_{72-87}^{i+7} and by alanine in Bak_{72-87}^{i+11}. In addition, Ile80 was changed to alanine in Bak_{72-87}^{i+11} to prevent possible steric clash with the crosslinker, and Ile81 was replaced with phenylalanine in both peptides because of the higher hydrophobicity of phenylalanine, which has been shown to increase the affinity of Bak_{72-87} for Bcl-x_L.[6] Similarly, a peptide based on proapoptotic Bid was designed to allow introduction of the azobenzene crosslinker for an *i*, *i*+4 spacing of the cysteines to generate Bid_{91-111}^{i+4}. Two methionine residues were substituted with isoleucine because of its higher stability towards oxidation. To produce the three photocontrollable peptide-based switches, Bak_{72-87}^{i+11}, Bak_{72-87}^{i+7}, and Bid_{91-111}^{i+4} were alkylated with 3,3′-bis(sulfo)-4,4′-bis(chloroacetamido)azobenzene.

Absorption spectroscopy

UV/Vis spectroscopy was used to characterize the thermal isomerization of irradiated Bak_{72-87}^{i+7}, Bak_{72-87}^{i+11}, and Bid_{91-111}^{i+4}. The absorption spectrum of dark-adapted Bak_{72-87}^{i+11}, in which the azobenzene crosslinker is in the thermally stable *trans*-configuration, was characterized by a strong maximum at 363 nm typical of the π–π* transitions in amide-substituted *trans*-azobenzenes (Figure 3).[46] Irradiation with 360 nm light led to the disappearance of this maximum and the appearance of a new maximum at 262 nm. Irradiated Bak_{72-87}^{i+11} reverted to the dark-adapted state in a nonphotochemical process characterized by isosbestic points at 250, 317, and 434 nm with a half-life of 22 min at 15 °C. This was similar to the half-life of FK-11, a previously reported peptide developed as a model system to test helix stabilization by crosslinkers,[36] but significantly shorter than the 150 min observed for the thermal reversion from the irradiated state of HDH-3, an 18-residue peptide derived from the homeobox protein engrailed linked to the azobenzene crosslinker in an *i*, *i*+11 configuration. The UV/Vis spectra of dark-adapted and irradiated Bak_{72-87}^{i+7} were similar to those observed for Bak_{72-87}^{i+11} (Supporting Information), but the thermal reversion from the irradiated states of Bak_{72-87}^{i+7} and Bid_{91-111}^{i+4} occurred with significantly longer half-lives of 174 and 190 min at 15 °C. Comparison of the reversion rates of Bak_{72-87}^{i+7} with those measured for Photo-MyoD ($\tau_{1/2}$ = 193 min at 15 °C)[35] and a synthetic peptide, designed for high helical propensity ($\tau_{1/2}$ = 37 min at 18 °C),[38] in which the crosslinkers were also in *i*, *i*+7

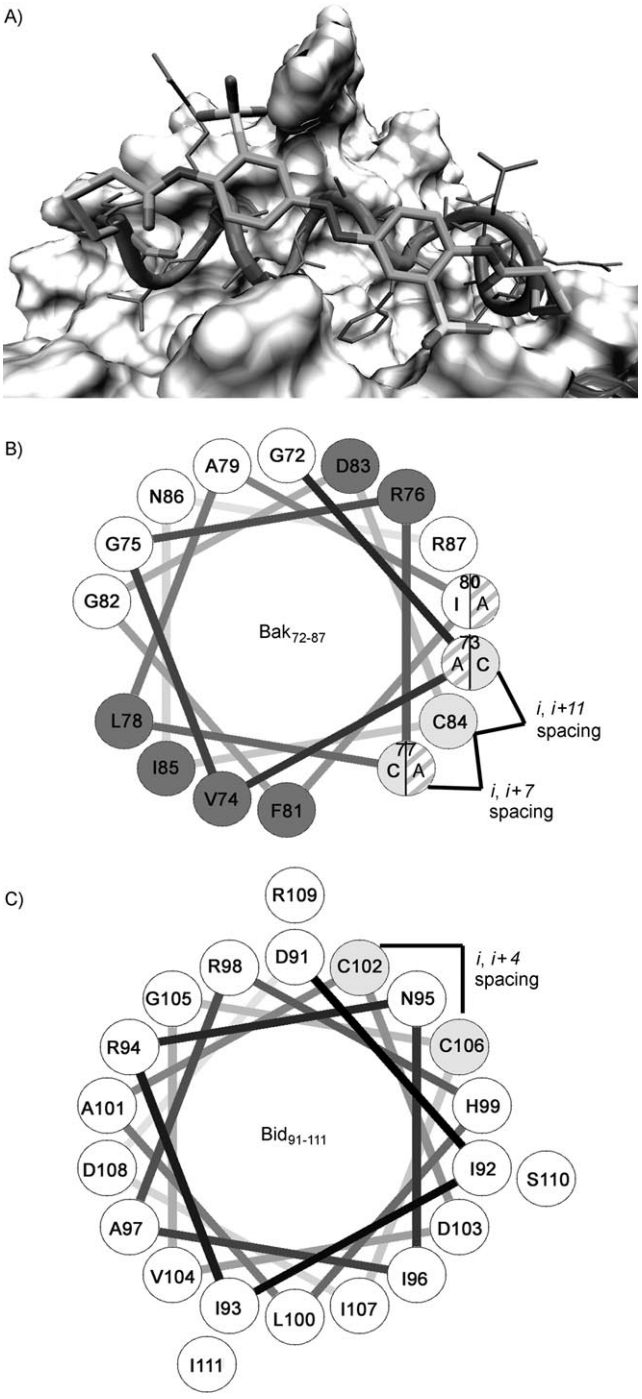

Figure 2. A) Model of Bak_{72-87}^{i+11} in complexation with Bcl-x_L. The model was generated from the structure of the complex with the wild-type Bak_{72-87} peptide.[23] Helical wheel representations of B) Bak_{72-87}^{i+7} and Bak_{72-87}^{i+11}, and C) Bid_{91-111}^{i+4}. Dark gray: residues shown to result in > tenfold loss of binding affinity for Bcl-x_L upon individual substitution with alanine. Light gray: cysteine residues introduced to allow crosslinking. Light gray stripes: residues replaced by an alanine unit to avoid steric clash with the azobenzene crosslinker. Where two labels are given for a single residue, the left-hand label refers to Bak_{72-87}^{i+7} and the right-hand label to Bak_{72-87}^{i+11}.

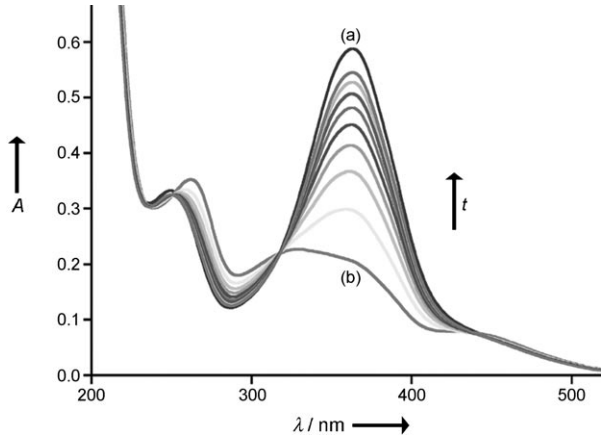

Figure 3. UV/Vis spectra of alkylated Bak_{72-87}^{i+11} at 5 °C. Spectra were acquired on a) the dark-adapted state, b) the irradiated state, and in 15-minute intervals after irradiation (15, 30, 45, 60, 75, 90, 105 and 120 min).

spacings, indicated that the rates of thermal reversion depend on both sequence and cysteine spacing.

The extent of light-induced isomerization was determined from the absorbance at 363 nm, by using the difference between the extinction coefficients for the *cis*- and *trans*-azobenzene crosslinkers;[36] 69%, 76%, and 80% of the irradiated material was found to be in the *cis* configuration for alkylated Bak_{72-87}^{i+11}, Bak_{72-87}^{i+7}, and Bid_{91-111}^{i+4}, respectively. These values are typically observed in the photoisomerization of azobenzenes.[34,47]

CD spectroscopy indicated significant differences in the conformations of noncrosslinked Bak_{72-87}^{i+11} and its alkylated dark-adapted form (Figure 4). The unalkylated peptide displayed the characteristic spectrum of a mostly unstructured peptide, with a minimum at 203 nm and mean residue ellipticity at 222 nm ($[\Theta]_{r,222}$) of -4752 deg cm^2 dmol^{-1} (Figure 4). For the *trans*-configuration of the crosslinker, the CD spectrum revealed almost complete helix formation with a $[\Theta]_{r,222}$ value of $-30\,600$ deg cm^2 dmol^{-1}. This value is significantly higher than had been observed previously for both HDH-3 and FK-11.[34,36] Interestingly, the mean residue ellipticity at 208 nm was higher ($-22\,250$ deg cm^2 dmol^{-1}), suggesting contributions to the CD spectrum from the crosslinker as previously described by Flint et al.[37] Irradiation with 360 nm light led to a significant increase in $[\Theta]_{r,222}$ to $-13\,458$ deg cm^2 dmol^{-1}, indicating a reduction in the amount of the peptide that adopts an α-helical structure as would have been predicted on the basis of previous studies.[34–40] Even in this state, however, the amount of α-helical character was approximately 44%, which is at least in part due to the presence in the irradiated state of Bak_{72-87}^{i+11} of approximately 31% of the *trans*-configured peptide (Figure 3).

In contrast, the CD spectra of alkylated Bak_{72-87}^{i+7} (Figure 4) and Bid_{91-111}^{i+4} (Supporting Information) were only slightly different in the dark-adapted and irradiated states. Both irradiated and dark-adapted Bak_{72-87}^{i+7} displayed only small amounts of α-helicity, with $[\Theta]_{r,222}$ values of -8808 and -6056 deg cm^2 dmol^{-1}, respectively. This is similar to the behavior previously reported for Photo-MyoD. In this case, DNA binding affinity could be modulated through an azobenzene linker introduced into the DNA recognition helix of MyoD by way of two cysteines in an *i*, *i*+7 spacing. Irradiated Photo-MyoD showed only a modest increase in α-helicity in relation

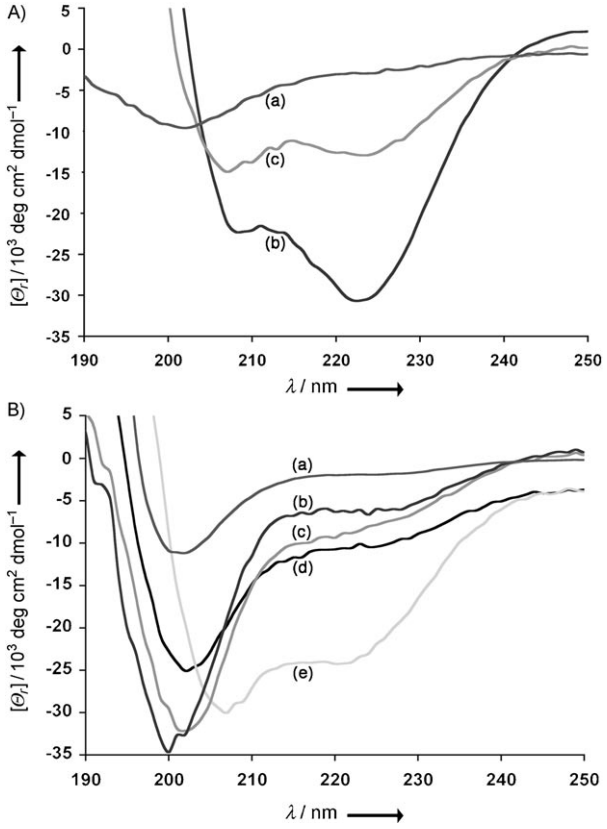

Figure 4. CD spectra of A) Bak_{72-87}^{i+11}, and B) Bak_{72-87}^{i+7} peptides at 5 °C. a) Unalkylated peptide, b) dark-adapted, c) irradiated, d) dark-adapted in 20% TFE, and e) irradiated in 20% TFE.

to its dark-adapted and unalkylated forms.[35] However, upon addition of the DNA target sequence, the full conformational change was induced.[35] Addition of Bcl-x_L to irradiated Bak_{72-87}^{i+7} and Bid_{91-111}^{i+4} may have a similar helix-inducing effect.

The dominant contribution from the elements of secondary structure of Bcl-x_L precluded us from studying this effect by CD spectroscopy. Hence, to probe the tendency of the peptides to adopt α-helical structures, 2,2,2-trifluoroethanol (TFE) was used as a co-solvent. This led to the typical CD spectra of predominantly α-helical peptides ($[\Theta]_{r,222}$ values of $-24\,100$ and $-17\,100$ deg cm^2 dmol^{-1} for irradiated Bak_{72-87}^{i+7} and Bid_{91-111}^{i+4}, respectively). Addition of TFE to solutions of either dark-adapted Bak_{72-87}^{i+7} or Bid_{91-111}^{i+4}, on the other hand, resulted in only marginal reductions in mean residue ellipticity. These observations suggest that although irradiation of Bak_{72-87}^{i+7} did not lead to a predominantly α-helical peptide, it nevertheless generated a form that upon addition of an α-helix-inducing cosolvent was able to form the α-helical structure required for tight binding to Bcl-x_L, while dark-adapted Bak_{72-87}^{i+7} did not have this potential.

Fluorescence polarization assays

Fluorescence anisotropy measurements[47] were carried out to determine the affinities of Bak_{72-87}^{i+11}, Bak_{72-87}^{i+7}, and Bid_{91-111}^{i+4} for Bcl-x_L in their non-crosslinked, dark-adapted, and light-induced states. The addition of Bcl-x_L to a solution of fluorescently labeled peptide resulted in a saturatable increase in the fluorescence anisotropy in each case (Figure 5). Titration curves were fitted to the Langmuir isotherm $\Phi_{Fit}=\{1+(K_D/[\text{Bcl-}x_L])^n\}^{-1}$. For all complexes, the best fits were obtained for 1:1 binding ($n=1$), as was expected from previous results with the wild-type peptide.[5,23,26,27] These fits yielded the apparent dissociation constants given in Table 1.

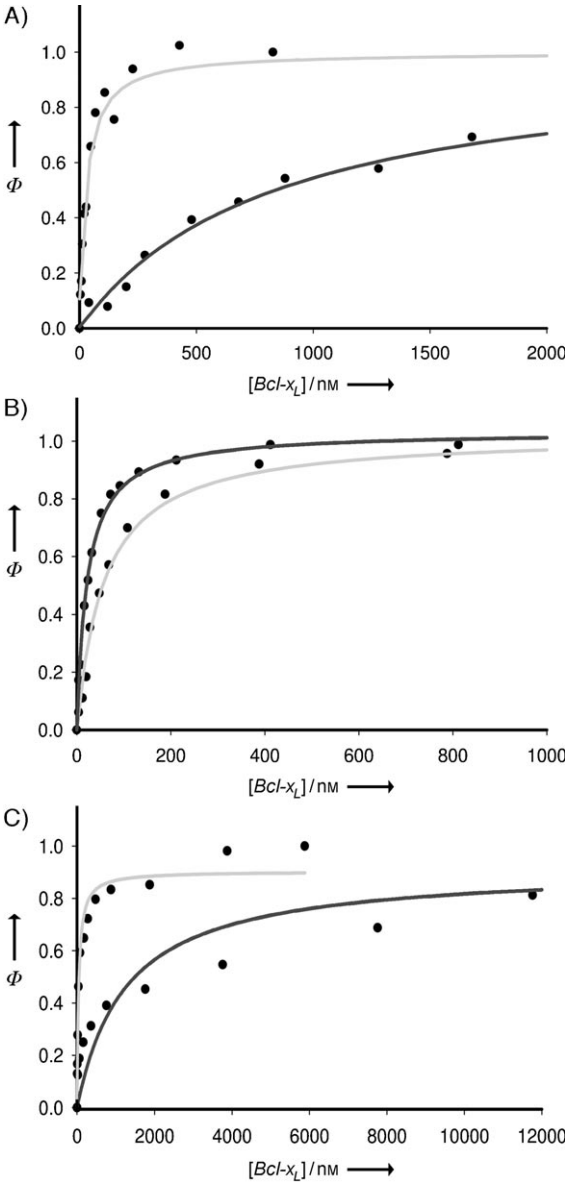

Figure 5. Typical binding curves for: A) Bak_{72-87}^{i+7}, B) Bak_{72-87}^{i+11}, and C) Bak_{91-111}^{i+4}. The black line in each case corresponds to the dark-adapted state, and the gray line to the irradiated state.

The dissociation constant for the complex of Bcl-x_L and dark-adapted Bak_{72-87}^{i+11} ($K_D=21\pm1$ nM) was ~16 times lower than that observed with the corresponding unalkylated peptide (Table 1). The K_D value of 328 ± 19 nM obtained for the unalkylated peptide is similar to values previously reported for wild-type Bak_{72-87}.[5,23] The stability of the Bcl-x_L complex of irradiat-

Table 1. Dissociation constants of the complexes of Bcl-x_L with Bak_{72-87}^{i+7}, Bak_{72-87}^{i+11}, and Bid_{91-111}^{i+4} in their parent (unalkylated), dark-adapted, and irradiated forms at 15 °C.

Peptide form	Bak_{72-87}^{i+7}	K_D [nM] Bak_{72-87}^{i+11}	Bid_{91-111}^{i+4}
parent	134 ± 16	328 ± 19	117 ± 48
dark-adapted	825 ± 157	21 ± 1	1275 ± 139
irradiated	42 ± 9	48 ± 10	55 ± 4

ed Bak_{72-87}^{i+11} was only decreased twofold relative to the complex with dark-adapted Bak_{72-87}^{i+11}. This high stability is most likely due to the incomplete *cis*- to *trans*-conversion of azobenzenes[36] and hence the presence of 31% tightly binding *trans*-configured peptide in the irradiated state (vide supra).

In contrast, both Bak_{72-87}^{i+7} and Bid_{91-111}^{i+4} showed significantly different complex stabilities in their dark-adapted and irradiated forms. For these two peptides, the *trans*-configuration of the crosslinker clearly prevented Bak_{72-87}^{i+7} ($K_D = 825 \pm 157$ nM) and Bid_{91-111}^{i+4} ($K_D = 1275 \pm 139$ nM) from forming high-affinity complexes (Table 1). These values were significantly higher than those measured for the unalkylated parent peptides of Bak_{72-87}^{i+7} and Bid_{91-111}^{i+4} ($K_D = 134 \pm 16$ nM and 117 ± 48 nM, respectively). After irradiation, the stabilities of the complexes formed between Bcl-x_L and the irradiated forms of Bak_{72-87}^{i+7} and Bid_{91-111}^{i+4} were increased approximately 20-fold, resulting in dissociation constants of 42 ± 9 and 55 ± 4 nM for the two peptides with the crosslinker in the helix-stabilizing *cis* configuration.

Bak_{72-87}^{i+11}, Bak_{72-87}^{i+7}, and Bid_{91-111}^{i+4} in their helix-stabilized forms bound to Bcl-x_L with much higher affinities than the wild-type peptides or helical peptide mimetics,[23,24,28,29,49] whereas the stabilities of the complexes of these peptides rivaled those of the best designed Bcl-x_L-targeting miniature proteins reported so far.[5,6,27] However, unlike peptides in which the α-helical conformation is stapled either through ruthenium-catalyzed olefin metathesis of tethered amino acids[16,27] or through their introduction into a larger stable polypeptide fold, such as pancreatic polypeptide,[5] the activities of the photocontrollable peptide-based switches described here can be switched between high and low Bcl-x_L affinity states with external light pulses.

A key issue for the potential use of photocontrollable peptide-based switches to regulate cellular events is whether they demonstrate selectivity between different helix-binding proteins. We therefore determined the abilities of alkylated Bak_{72-87}^{i+11}, Bak_{72-87}^{i+7}, and Bid_{91-111}^{i+4} to bind to Hdm2, a target of the tumor suppressor p53.[50] The stability of the complex between Hdm2 and p53 is the consequence of an α-helix of p53 binding to a deep cleft on the surface of Hdm2.[51] However, no binding activity for Hdm2 was detected here in fluorescence anisotropy measurements for dark-adapted and irradiated Bak_{72-87}^{i+11}, Bak_{72-87}^{i+7}, and Bak_{91-111}^{i+4} at concentrations up to 10 μM, indicating that the selectivity was more than 200-fold in their helical state.

Chemical shift perturbation measurements

To determine whether dark-adapted Bak_{72-87}^{i+11} interacted with the binding groove of Bcl-x_L, ^1H–^{15}N heteronuclear single-quantum correlation (HSQC) NMR spectra were measured for free ^{15}N-labeled Bcl-x_L and complexes with wild-type Bak_{72-87} and dark-adapted Bak_{72-87}^{i+11}. For these studies, Bcl-x_L 1–212 (Δ45–84), which lacks the flexible loop between residues 45 and 84, was used. Previous studies have shown that this truncated version of Bcl-x_L has the same anti-apoptotic and peptide binding activities as Bcl-x_L 1–212.[23,52] The HSQC spectra show comparable chemical shift changes, indicating that the structural changes of Bcl-x_L upon addition of dark-adapted Bak_{72-87}^{i+11} are very similar to those obtained with wild-type Bak_{72-87} (Figure 6). The resonances in the HSQC spectrum for the complex of Bcl-x_L with dark-adapted Bak_{72-87}^{i+11} were assigned from a HSQC-TOCSY spectrum and by comparison with the published assignments for the complex of Bcl-x_L with a 25-residue peptide corresponding to the BH3 helix of the proapoptotic protein Bad.[24]

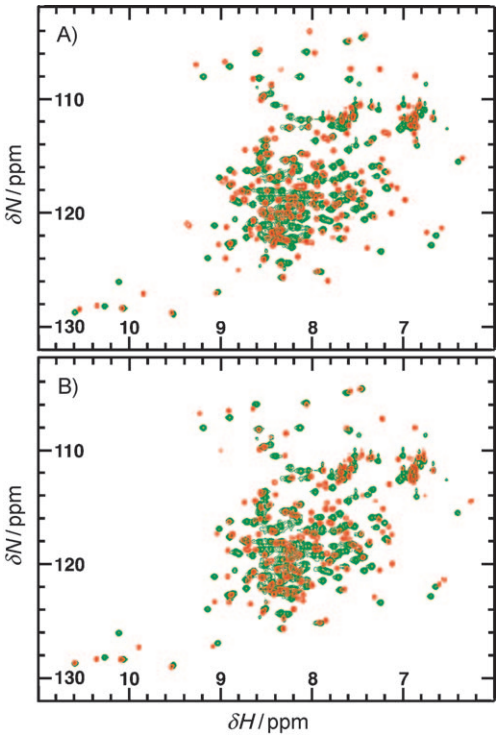

Figure 6. ^1H–^{15}N HSQC NMR spectra of free Bcl-x_L 1–212 (Δ45–84, green) and in complexation (red) with A) wild-type Bak_{72-87}, and B) dark-adapted alkylated Bak_{72-87}^{i+11}.

Complexation with dark-adapted Bak_{72-87}^{i+11} led to chemical shift changes in most residues of Bcl-x_L (Supporting Information). Residues F57, E58, F65, T69, S82, F91, D93, G94, W97, F106, T132, and Y133 in particular showed strong changes in their chemical shifts (shown in red in Figure 7). These residues lie in the region of Bcl-x_L that had previously been defined as forming the binding cleft for Bak and Bad.[23,24] Many other residues showed medium chemical shift changes on binding to

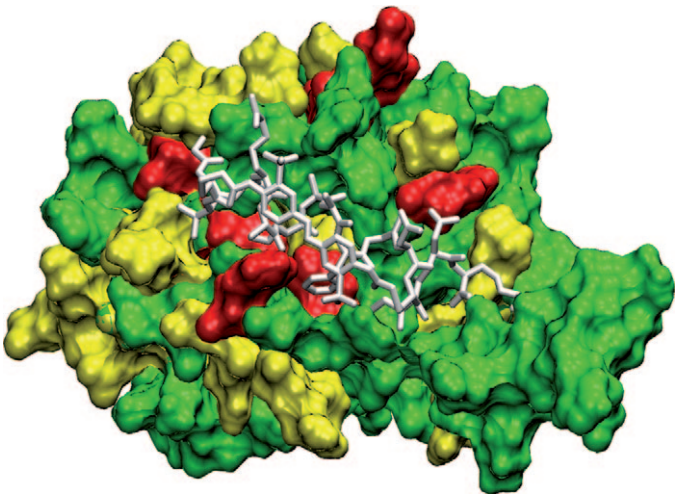

Figure 7. Surface representation of Bcl-x_L showing residues that undergo changes in NH chemical shift upon binding to Bak_{72-87}^{i+11}. Minimum chemical shift changes were mapped onto the model of the Bcl-x_L/Bak_{72-87}^{i+11} complex. Red: $\omega > 0.4\omega_{max}$. Yellow: $0.4\omega_{max} > \omega > 0.15\omega_{max}$. Green: $\omega < 0.15\omega_{max}$. The modeled Bak_{72-87}^{i+11} peptide is shown as white sticks.

dark-adapted Bak_{72-87}^{i+11} (shown in yellow in Figure 7). While residues Q71, L72, Q85, A102, and L154 were in the direct vicinity of the binding cleft on Bcl-x_L and hence further confirmed that Bak_{72-87}^{i+11} bound to this region, several residues further away from the binding cleft also showed medium chemical shift changes, in agreement with a previous report in which such long-range inductive effects had also been observed.[53] These data indicated strongly that dark-adapted Bak_{72-87}^{i+11} and wild-type Bak_{72-87} target the same area on the surface of Bcl-x_L.

Interestingly, the HSQC spectrum of Bcl-x_L in complexation with Bak_{72-87}^{i+7} (Supporting Information) was almost identical to that of the complex with Bak_{72-87}^{i+11}. In the dark-adapted state, Bak_{72-87}^{i+7} adopts a largely disordered structure and binds Bcl-x_L weakly, whereas Bak_{72-87}^{i+11} is predominantly helical and binds Bcl-x_L more strongly (vide supra). The strong similarities between the HSQC spectra of the two complexes therefore show that isomerization of the crosslinker affects only the affinity of the peptide for Bcl-x_L, rather than its preferred binding site.

Conclusions

In summary, a family of photocontrollable peptide-based switches that target the anti-apoptotic protein Bcl-x_L has been developed, through the use of an azobenzene-derived photoactivatable crosslinker to regulate the conformation of short peptides based on the BH3 regions of the Bcl-x_L-binding proteins Bak[23] and Bid.[27] The binding mode was determined by CD and NMR spectroscopy, which revealed that these peptides bind to the same cleft of Bcl-x_L that had been identified as the target site of wild-type Bak and Bid. However, helix-stabilized peptides showed significantly greater affinities for Bcl-x_L than the unalkylated and wild-type peptides, whereas the helix-destabilized forms generally showed reduced affinity. The availability of such peptides should in the future provide the opportunity to activate apoptotic process in cellular systems through the application of external light pulses.

The technology described here has a high level of generic character, because many other protein–protein interactions depend on α-helices. In addition, it can be extended to control the conformation of β-strands. Applications in surface chemistry, imaging, particle physics, and medical diagnostics could also be envisaged. The combined features of high affinity and high specificity together with their stable peptide fold suggest that these and similar peptides might be used to probe and modulate specific protein function within the context of the cellular proteome. While other peptide-based and small molecule reagents have been developed to target specific protein–protein interactions, our peptide-based switches are unique in that their protein-binding activity can be controlled externally by irradiation with light, opening the possibility of interfering specifically with such interactions to study and modulate cellular function.

Experimental Section

Peptide synthesis and purification: All peptides were synthesized by solid-phase peptide synthesis on a CEM peptide synthesizer (Matthews, NC, USA), by standard 9-fluorenylmethoxycarbonyl (Fmoc) group chemistry protocols. The C-termini were produced in their amidated forms, and the N-terminal amines were acetylated or labeled with carboxyfluorescein (FAM) for fluorescence anisotropy measurements. Wild-type Bak_{72-87} and Bak_{72-87}^{i+7} were synthesized on Rink amide resins. Bak_{72-87}^{i+11} and Bak_{91-111}^{i+4} were synthesized on Rink amide 4-methylbenzhydrylamine resins. For FAM-labeling, the resin-bound peptide was incubated at room temperature with FAM (50 mg), *N*-hydroxybenzotriazole (20 mg), and diisopropylcarbodiimide (26 μL) in DMF (1.5 mL) for 2 h prior to cleavage from the resin with TFA. Crude peptides were dissolved in acetonitrile/water (1:1) and purified by reversed-phase HPLC on a Phenomenex Luna 10 μm C18 100 Å column (250×10 mm; Torrance, CA, USA) at a flow rate of 5 mL min^{-1}. A linear 0–60% acetonitrile gradient was run over 60 min. Peptide concentrations were obtained from absorbance at 210 nm ($\varepsilon = 20$ mL mg^{-1} cm^{-1}).[54] Concentrations of FAM-labeled peptides were determined at 494 nm ($\varepsilon = 83\,000$ M^{-1} cm^{-1}).[34]

Peptide alkylations: The crosslinker 3,3′-bis(sulfo)-4,4′-bis(chloroacetamido)azobenzene was synthesized as described previously.[36] All reactions involving the crosslinker were performed in the dark. The peptide (1 mg) was fully reduced prior to alkylation by incubation in Tris buffer (pH 8.3, 50 mM, 1 mL) containing tris(carboxyethyl)phosphine (TCEP, 0.5 mM) at 4 °C for 15 min. For Bak_{72-87} peptides, crosslinker solution (2 mM) in Tris buffer (pH 8.3, 50 mM) was added to the reduced peptide in three 333 μL portions at 20 min intervals. After 12 h the alkylated peptides were purified by reversed-phase HPLC as described above. The alkylation reaction for Bak_{91-111}^{i+4} was performed at 50 °C with 2 h incubation after each addition of the azobenzene. The elevated temperature and increased reaction time were required because under the conditions used for the Bak peptides, bis-alkylation of Bak_{91-111}^{i+4} with two azobenzene moieties was observed rather than crosslinking with a single azobenzene. This is likely to be due to the close proximity of the reactive thiols, which disfavors intramolecular alkylation. By decreasing the degree of peptide structure, elevated temperatures may increase this distance and so favor intramolecular reaction. Purifica-

tion was performed immediately afterwards as described for Bak_{72-87} peptides. Concentrations of alkylated peptides were calculated with an extinction coefficient at 363 nm of 24000 $M^{-1}cm^{-1}$.[34]

Photoisomerization: Dark-adapted peptide-based switches were photoisomerized by irradiating the peptide solution (typically 100 μM) for 4 min with a 250 W metal halide UV light point source (UV-P280, Panacol–Elosol, GmbH, Oberursel, Germany) coupled to a 360 nm band-pass filter.

Purification of Bcl-x_L and Hdm2: A plasmid containing the cDNA for Hdm2 residues 1–188 was obtained from David Lane (University of Dundee, UK). A fragment encoding amino acids 1–125 was expressed in *E. coli* and purified as previously described.[55] A plasmid encoding human Bcl-x_L was obtained from Marion McFarlane (University of Leicester, UK). The gene encoding Bcl-x_L was amplified by PCR with use of the primers bcl-x_L fwd; 5′-GTA CGC ATA TGT CTC AGA GCA ACC GGG AGC-3′ and bcl-x_L rev; 5′-CTA GTA GAT CTT CAG CGT TCC TGG CCC TTT CG-3′, designed to introduce NdeI and BglII restriction sites (sequences underlined) flanking the gene and to delete the C-terminal domain of the protein. The PCR product was cloned into a PCR-Script vector using blunt end ligation. The resulting plasmid was digested with the NdeI and BglII restriction enzymes, and the 639 bp fragment coding for amino acids 1–212 of Bcl-x_L was introduced into the NdeI and BamHI digested pET19b expression vector, which codes for a N-terminal His-tag. DNA sequencing confirmed the presence and correct sequence of the bcl-x_L insert. This pET19b-bcl-x_L (1–212) expression vector was transformed into *E. coli* BL21(DE3) cells, which were grown at 37 °C in LB medium to an OD_{600} of 0.5 and expression induced with isopropyl β-D-galactopyranoside (IPTG, 0.4 mM). Six hours after IPTG addition the cells were harvested, resuspended in sodium phosphate buffer (pH 7.5, 100 mM) containing β-mercaptoethanol (100 mM), and lyzed by sonication. Cell debris was removed by centrifugation at 40000 g for 20 min, and the clarified lysate was dialyzed against sodium phosphate buffer (pH 7.5, 100 mM) containing β-mercaptoethanol (5 mM) to allow purification on a Ni-sepharose column. After loading the protein solution, the column was washed with sodium phosphate buffer (pH 7.5, 100 mM) containing NaCl (500 mM), β-mercaptoethanol (5 mM), and imidazole (50 mM), and bound Bcl-x_L was eluted with the same buffer containing imidazole (500 mM). The purity of the resulting 26 kDa protein was analyzed by SDS polyacrylamide gel electrophoresis (Supporting Information) and the correct mass was verified by MALDI-TOF mass spectrometry (measured: 25922 Da; calculated: 25985 Da). The yield of pure protein was 30 mg L^{-1} of culture. For NMR experiments, truncated-loop Bcl-x_L was used because of its lower aggregation tendency. A pET vector encoding residues 1–212 (Δ45–84) of Bcl-x_L with a C-terminal His-tag was transformed into *E. coli* BL21(DE3) cells, which were grown at 37 °C in M9 minimal medium containing $^{15}NH_4Cl$. The protein was prepared as described for non-truncated Bcl-x_L. MALDI-TOF mass spectrometry showed a peak at *m/z* 21428, in good agreement with the expected mass of 21567 Da for the labeled protein.

UV/Vis spectroscopy: All spectra were recorded in potassium phosphate buffer (pH 8.0, 5 mM) at 5 °C with a Shimadzu UV-2401PC UV-Vis spectrometer in a 5 mm or 1 mm pathlength cuvette. The concentration of Bak_{72-87}^{i+11} was 250 μM. First-order kinetics for the thermal *cis*- to *trans*-reversion were assumed, because the rate of reversion should only depend on the concentration of *cis*-peptide (*cis*-P). The corresponding integrated first-order rate law is given in Equation (1):

$$[cis\text{-P}] = [cis\text{-P}]_0\, e^{-kt} \quad (1)$$

Since [*cis*-P] is directly proportional to the percentage of non-reverted irradiated peptide ($\%_{irrad}$), the rate constant (*k*) for the thermal relaxation process could be calculated from a plot of $\ln \%_{irrad}(t)$ versus t $\%_{irrad}(t)$ is defined in Equation (2):

$$\%\ \text{irrad}\ (t) = 100\, A_{363}(t)/(A_{363}^{dark} - A_{363}^{irrad}) \quad (2)$$

where $A_{363}(t)$ is the measured absorbance at 363 nm at time *t*, and A_{363}^{dark} and A_{363}^{irrad} are the values for the absorbance immediately before and after irradiation.

Circular dichroism spectroscopy: All spectra were recorded in potassium phosphate buffer (pH 8.0, 5 mM) in a 1 mm pathlength cuvette at 5 °C with an Applied Photophysics Chirascan spectrometer. The peptide concentration was typically 100 μM. Spectra were also acquired in the presence of 2,2,2-trifluoroethanol (20%), which promotes helix formation.[56] Mean residue ellipticities were calculated according to Equation (3):

$$[\Theta]_r = \Theta/(10\, ncl) \quad (3)$$

where Θ is the measured ellipticity in mdeg, *n* is the number of backbone amide bonds, *c* is the concentration in M, and *l* is the pathlength in cm. The percentage helical structure was calculated from Equation (4):

$$\%\ \text{helicity} = -100\, n\ [\Theta]_{r,222}/40000\ (n-4) \quad (4)$$

where *n* is the number of amide bonds in the peptide.[36]

Binding experiments using fluorescence anisotropy measurements: Fluorescence anisotropy measurements were carried out on a Perkin–Elmer LS55 luminescence spectrometer at 15 °C (excitation at 494 nm and emission at 525 nm; slit width 5 nm, integration time 5 s). All measurements were performed in a 1 mL fluorescence quartz cuvette with FAM-labeled peptide (10 nM). The assay was performed in sodium phosphate buffer (pH 7.5, 100 mM) containing NaCl (10 mM). Defined volumes of Bcl-x_L solution (4 μM or 40 μM) were added to the FAM-labeled peptide, and the changes in fluorescence anisotropy were measured. For experiments using light-induced peptides the solution in the cuvette was re-irradiated for 30 s every 5 min to keep the maximum amount of azobenzene crosslinker in the *cis* form. The *G* factor (ratio of monochromator sensitivity for horizontally and vertically polarized light) was calculated for each measurement by Equation (5)

$$G = I_\perp/I_\parallel \quad (5)$$

where $I_\parallel$ and $I_\perp$ are the intensities of the fluorescence emission in planes parallel and perpendicular, respectively, to the excitation plane. Values for fluorescence anisotropy (*A*) were then determined from Equation (6)[48]

$$A = (I_\parallel - GI_\perp/I_\parallel + 2\, GI_\perp) \quad (6)$$

The fraction of bound peptide (Φ) was derived by normalizing the anisotropy data. The resultant Φ values were fitted to the Langmuir equation [Eq. (7)] with use of the program Sigmaplot to obtain K_D

$$\Phi_{Fit} = \{1 + (K_D/[\text{Bcl-x}_L])^n\}^{-1} \quad (7)$$

All binding curves were acquired independently four times, and the resulting K_D values were averaged. Errors are standard errors of the mean at 2σ.

NMR experiments: All NMR experiments were performed in sodium phosphate buffer (pH 7.3, 10 mM) containing β-mercaptoethanol (5 mM). ^{15}N-Labeled Bcl-x_L was concentrated to 300 μM, and D_2O (5%, *v/v*) was added. ^{1}H–^{15}N HSQC spectra of free Bcl-x_L and its complexes with unlabeled wild-type Bak_{72-87} and dark-adapted Bak_{72-87}^{i+7} and Bak_{72-87}^{i+11} (1:1.1 protein to peptide ratio) were acquired on a Varian INOVA 600 MHz NMR spectrometer. For the complex with dark-adapted Bak_{72-87}^{i+11}, a ^{1}H–^{15}N HSQC-TOCSY spectrum was also acquired. Spectra were processed by use of NMRPipe[57] and analyzed by using the Analysis 1.0.15 software for Linux.[58] HSQC peaks for the complex with dark-adapted Bak_{72-87}^{i+11} were assigned by comparison with the published assignments for the Bcl-x_L/Bad complex,[24] and assignment of residue types were verified by use of a three-dimensional ^{15}N-edited HSQC-TOCSY spectrum. When ^{1}H–^{15}N HSQC spectra of uncomplexed and complexed Bcl-x_L were compared, peak movements were calculated by use of Eq. (8):

$$\omega = \{(\Delta(\delta H))^2+(\Delta(\delta N)/5)^2\}^{1/2} \quad (8)$$

and were expressed as fractions of the maximum peak movements. A significant change in chemical shift was defined as $\omega > 0.4\,\omega_{max}$.

Modeling of the complex of dark-adapted-Bak_{72-87}^{i+11} and Bcl-x_L: The model was generated from the NMR structure of the complex of Bcl-x_L and wild-type Bak_{72-87} (PDB 1BXL)[23] by use of the Molecular Operating Environment software for Linux. After the necessary amino acid substitutions and incorporation of the crosslinker, the forcefield MMFF94[59] was used to minimize the energy of the peptide and a 4.5 Å region around it.

Acknowledgements

We thank Dr. Marion MacFarlane of the Medical Research Council Toxicology Unit at the University of Leicester for providing us with a cDNA for Bcl-x_L and Prof. Sir David Lane of the University of Dundee for providing us with a cDNA for Hdm2. The help of Piotr Wysoczanski and Thomas Fricke is gratefully acknowledged. The UK Biotechnology and Biological Sciences Research Council (BBSRC) (R.K.A.), Wellcome Trust (C.W.), and Cardiff University (studentship to S.K.) supported this work.

Keywords: apoptosis · azobenzenes · BH3 domain · photochemistry · protein–protein interactions

[1] R. Prasad Bahadur, P. Chakrabarti, F. Rodier, J. Janin, *J. Mol. Biol.* **2004**, *336*, 943.
[2] I. M. Nooren, J. M. Thornton, *J. Mol. Biol.* **2003**, *325*, 991.
[3] D. Reichmann, O. Rahat, S. Albeck, R. Meged, O. Dym, G. Schreiber, *Proc. Natl. Acad. Sci. USA* **2005**, *102*, 57.
[4] D. Reichmann, O. Rahat, M. Cohen, H. Neuvirth, G. Schreiber, *Curr. Opin. Struct. Biol.* **2007**, *17*, 67.
[5] A. C. Gemperli, S. E. Rutledge, A. Maranda, A. Schepartz, *J. Am. Chem. Soc.* **2005**, *127*, 1596.
[6] J. W. Chin, A. Schepartz, *Angew. Chem.* **2001**, *113*, 3922; *Angew. Chem. Int. Ed.* **2001**, *40*, 3806.
[7] S. E. Rutledge, J. W. Chin, A. Schepartz, *Curr. Opin. Chem. Biol.* **2002**, *6*, 479.
[8] S. E. Rutledge, H. M. Volkman, A. Schepartz, *J. Am. Chem. Soc.* **2003**, *125*, 14336.
[9] K. Sakurai, H. S. Chung, D. Kahne, *J. Am. Chem. Soc.* **2004**, *126*, 16288.
[10] J. A. Kritzer, J. D. Lear, M. E. Hodsdon, A. Schepartz, *J. Am. Chem. Soc.* **2004**, *126*, 9468.
[11] J. A. Kritzer, O. M. Stephens, D. A. Guarracino, S. K. Reznik, A. Schepartz, *Bioorg. Med. Chem.* **2005**, *13*, 11.
[12] J. A. Kritzer, R. Zutshi, M. Cheah, F. A. Ran, R. Webman, T. M. Wongjirad, A. Schepartz, *ChemBioChem* **2006**, *7*, 29.
[13] H. M. Volkman, S. E. Rutledge, A. Schepartz, *J. Am. Chem. Soc.* **2005**, *127*, 4649.
[14] K. J. Oh, S. Barbuto, K. Pitter, J. Morash, L. D. Walensky, S. J. Korsmeyer, *J. Biol. Chem.* **2006**, *281*, 36999.
[15] A. VanderBorght, A. Valckx, J. Van Dun, T. Grand-Perret, S. De Schepper, J. Vialard, M. Janicot, J. Arts, *Oncogene* **2006**, *25*, 6672.
[16] F. Bernal, A. F. Tyler, S. J. Korsmeyer, L. D. Walensky, G. L. Verdine, *J. Am. Chem. Soc.* **2007**, *129*, 2456.
[17] J. H. Holtzman, K. Woronowicz, D. Golemi-Kotra, A. Schepartz, *Biochemistry* **2007**, *46*, 13541.
[18] S. Cory, D. C. Huang, J. M. Adams, *Oncogene* **2003**, *22*, 8590.
[19] R. Kim, *Biochem. Biophys. Res. Commun.* **2005**, *333*, 336.
[20] T. Chittenden, E. A. Harrington, R. O'Connor, C. Flemington, R. J. Lutz, G. I. Evan, B. C. Guild, *Nature* **1995**, *374*, 733.
[21] K. Wang, X. M. Yin, D. T. Chao, C. L. Milliman, S. J. Korsmeyer, *Genes Dev.* **1996**, *10*, 2859.
[22] M. O. Hengartner, *Nature* **2000**, *407*, 770.
[23] M. Sattler, H. Liang, D. Nettesheim, R. P. Meadows, J. E. Harlan, M. Eberstadt, H. S. Yoon, S. B. Shuker, B. S. Chang, A. J. Minn, C. B. Thompson, S. W. Fesik, *Science* **1997**, *275*, 983.
[24] A. M. Petros, D. G. Nettesheim, Y. Wang, E. T. Olejniczak, R. P. Meadows, J. Mack, K. Swift, E. D. Matayoshi, H. Zhang, C. B. Thompson, S. W. Fesik, *Protein Sci.* **2000**, *9*, 2528.
[25] O. Kutzki, H. S. Park, J. T. Ernst, B. P. Orner, H. Yin, A. D. Hamilton, *J. Am. Chem. Soc.* **2002**, *124*, 11838.
[26] J. T. Ernst, J. Becerril, H. S. Park, H. Yin, A. D. Hamilton, *Angew. Chem.* **2003**, *115*, 553; *Angew. Chem. Int. Ed.* **2003**, *42*, 535.
[27] L. D. Walensky, A. L. Kung, I. Escher, T. J. Malia, S. Barbuto, R. D. Wright, G. Wagner, G. L. Verdine, S. J. Korsmeyer, *Science* **2004**, *305*, 1466.
[28] H. Yin, A. D. Hamilton, *Bioorg. Med. Chem. Lett.* **2004**, *14*, 1375.
[29] H. Yin, G. I. Lee, K. A. Sedey, O. Kutzki, H. S. Park, B. P. Orner, J. T. Ernst, H. G. Wang, S. M. Sebti, A. D. Hamilton, *J. Am. Chem. Soc.* **2005**, *127*, 10191.
[30] T. Oltersdorf, S. W. Elmore, A. R. Shoemaker, R. C. Armstrong, D. J. Augeri, B. A. Belli, M. Bruncko, T. L. Deckwerth, J. Dinges, P. J. Hajduk, M. K. Joseph, S. Kitada, S. J. Korsmeyer, A. R. Kunzer, A. Letai, C. Li, M. J. Mitten, D. G. Nettesheim, S. Ng, P. M. Nimmer, J. M. O'Connor, A. Oleksijew, A. M. Petros, J. C. Reed, W. Shen, S. K. Tahir, C. B. Thompson, K. J. Tomaselli, B. Wang, M. D. Wendt, H. Zhang, S. W. Fesik, S. H. Rosenberg, *Nature* **2005**, *435*, 677.
[31] R. M. Mohammad, S. Wang, S. Banerjee, X. Wu, J. Chen, F. H. Sarkar, *Pancreas* **2005**, *31*, 317.
[32] M. Bruncko, T. K. Oost, B. A. Belli, H. Ding, M. K. Joseph, A. Kunzer, D. Martineau, W. J. McClellan, M. Mitten, S. C. Ng, P. M. Nimmer, T. Oltersdorf, C. M. Park, A. M. Petros, A. R. Shoemaker, X. Song, X. Wang, M. D. Wendt, H. Zhang, S. W. Fesik, S. H. Rosenberg, S. W. Elmore, *J. Med. Chem.* **2007**, *50*, 641.
[33] M. Zhang, Y. Ling, C. Y. Yang, H. Liu, R. Wang, X. Wu, K. Ding, F. Zhu, B. N. Griffith, R. M. Mohammad, S. Wang, D. Yang, *Ann. Hematol.* **2007**, *86*, 471.
[34] L. Guerrero, O. S. Smart, G. A. Woolley, R. K. Allemann, *J. Am. Chem. Soc.* **2005**, *127*, 15624.
[35] L. Guerrero, O. S. Smart, C. J. Weston, D. C. Burns, G. A. Woolley, R. K. Allemann, *Angew. Chem.* **2005**, *117*, 7956; *Angew. Chem. Int. Ed.* **2005**, *44*, 7778.
[36] Z. Zhang, D. C. Burns, J. R. Kumita, O. S. Smart, G. A. Woolley, *Bioconjugate Chem.* **2003**, *14*, 824.
[37] D. G. Flint, J. R. Kumita, O. S. Smart, G. A. Woolley, *Chem. Biol.* **2002**, *9*, 391.
[38] J. R. Kumita, O. S. Smart, G. A. Woolley, *Proc. Natl. Acad. Sci. USA* **2000**, *97*, 3803.
[39] G. A. Woolley, A. S. Jaikaran, M. Berezovski, J. P. Calarco, S. N. Krylov, O. S. Smart, J. R. Kumita, *Biochemistry* **2006**, *45*, 6075.
[40] J. R. Kumita, D. G. Flint, G. A. Woolley, O. S. Smart, *Faraday Discuss.* **2003**, *122*, 89.

[41] U. Kusebauch, S. A. Cadamuro, H. J. Musiol, L. Moroder, C. Renner, *Chem. Eur. J.* **2007**, *13*, 2966.
[42] A. M. Caamaño, M. E. Vásquez, J. Martínez-Costas, L. Castedo, J. L. Mascareñas, *Angew. Chem.* **2000**, *112*, 3234; *Angew. Chem. Int. Ed.* **2000**, *39*, 3104.
[43] A. Aemissegger, V. Krautler, W. F. van Gunsteren, D. Hilvert, *J. Am. Chem. Soc.* **2005**, *127*, 2929.
[44] S. L. Dong, M. Loweneck, T. E. Schrader, W. J. Schreier, W. Zinth, L. Moroder, C. Renner, *Chem. Eur. J.* **2006**, *12*, 1114.
[45] T. E. Schrader, W. J. Schreier, T. Cordes, F. O. Koller, G. Babitzki, R. Denschlag, C. Renner, M. Loweneckt, S. L. Dong, L. Moroder, P. Tavan, W. Zinth, *Proc. Natl. Acad. Sci. USA* **2007**, *104*, 15729.
[46] H. Rau in *Photoisomerization of Azobenzenes*, CRC Press, Boca Raton, **1990**, pp. 119.
[47] C. Renner, L. Moroder, *ChemBioChem* **2006**, *7*, 868.
[48] T. Heyduk, Y. Ma, H. Tang, R. H. Ebright, *Methods Enzymol.* **1996**, *274*, 492.
[49] H. Yin, G. Lee, H. S. Park, G. A. Payne, J. M. Rodriguez, S. M. Sebti, A. D. Hamilton, *Angew. Chem.* **2005**, *117*, 2764; *Angew. Chem. Int. Ed.* **2005**, *44*, 2704.
[50] A. C. Joerger, A. R. Fersht, *Oncogene* **2007**, *26*, 2226.
[51] P. H. Kussie, S. Gorina, V. Marechal, B. Elenbaas, J. Moreau, A. J. Levine, N. P. Pavletich, *Science* **1996**, *274*, 948.
[52] T. Sato, M. Hanada, S. Bodrug, S. J. Irie, N. Iwama, L. H. Boise, C. B. Thompson, E. Golemis, L. Fong, H. G. Wang, J. C. Reed, *Proc. Natl. Acad. Sci. USA* **1994**, *91*, 9238.
[53] W. Feng, S. Huang, H. Wu, M. Zhang, *J. Mol. Biol.* **2007**, *372*, 223.
[54] D. B. Wetlaufer, *Adv. Prot. Chem.* **1963**, *17*, 303.
[55] V. Bottger, A. Bottger, S. F. Howard, S. M. Picksley, P. Chene, C. G. Echeverria, H. K. Hochkeppel, D. P. Lane, *Oncogene* **1996**, *13*, 2141.
[56] R. W. Storrs, D. Truckses, D. E. Wemmer, *Biopolymers* **1992**, *32*, 1695.
[57] F. Delaglio, S. Grzesiek, G. W. Vuister, G. Zhu, J. Pfeifer, A. Bax, *J. Biomol. NMR* **1995**, *6*, 277.
[58] W. F. Vranken, W. Boucher, T. J. Stevens, R. H. Fogh, A. Pajon, M. Llinas, E. L. Ulrich, J. L. Markley, J. Ionides, E. D. Laue, *Proteins Struct. Funct. Bioinf.* **2005**, *59*, 687.
[59] T. A. Halgren, *J. Comput. Chem.* **1996**, *17*, 490.

Received: July 22, 2008
Published online on November 14, 2008

